Arctic, Antarctic, and Alpine Research, Vol. 48, No. 2, 2016, pp. 263–277
DOI: http://dx.doi.org/10.1657/AAAR0015-059

Calving behavior at Rink Isbræ, West Greenland, from time-lapse photos

Dorota Medrzycka[1,*], Douglas I. Benn[2,3], Jason E. Box[4], Luke Copland[1], and James Balog[5]

[1]Department of Geography, Environment and Geomatics, University of Ottawa, Ottawa, Ontario, K1N 6N5, Canada
[2]School of Geography and Geosciences, University of St Andrews, St Andrews KY16 9AL, U.K.
[3]Department of Arctic Geology, University Centre in Svalbard, N-9171 Longyearbyen, Norway
[4]Department of Marine Geology and Glaciology, Geological Survey of Denmark and Greenland, DK-1350 Copenhagen, Denmark
[5]Earth Vision Institute, 2334 Broadway, Boulder, Colorado 80304, U.S.A.
[*]Corresponding author: dorota.medrzycka@uottawa.ca

A B S T R A C T

This study presents detailed observations of calving behavior variability from daily oblique photographs acquired over a five-year period (2007–2011) covering the terminus of Rink Isbræ, a major West Greenland outlet glacier. The evidence suggests that calving at Rink is characterized by two styles with distinct temporal and spatial footprints. The first style is characterized by frequent small magnitude events, which show clear seasonal variability with a marked increase in frequency immediately following ice mélange breakup and a peak in July. The second style is characterized by the sporadic detachment of kilometer-sized tabular icebergs with no clear seasonal signal. We suggest that two sets of mechanisms control calving variability at this location, namely (1) melt-driven processes enhancing submarine undercutting and (2) mechanically driven buoyant flexure. The presence of sea ice and/or ice mélange in the fjord presents an additional factor limiting calving in the winter.

Introduction

Recent studies indicate that the dynamics of marine-terminating glaciers are sensitive to changes in boundary conditions at the terminus. Feedbacks between calving and ice dynamics imply a strong coupling between processes acting at the ice margins and changes upglacier (Joughin et al., 2004; Thomas, 2004; Howat et al., 2005; Joughin et al., 2008c; Nick et al., 2009; Vieli and Nick, 2011). Studies focusing on individual calving events suggest that rapid and localized perturbations may additionally determine the location, magnitude, and timing of events (O'Neel et al., 2003, 2005, 2007; Bassis and Jacobs, 2013; Chapuis and Tetzlaff, 2014). Short-term terminus stability is therefore dependent on several parameters modifying boundary conditions at the ice cliffs, including atmospheric and oceanic factors, the presence of sea ice/ice mélange in the fjord, as well as glacier specific factors such as ice thickness and fjord bathymetry. For this reason, and due to the wide range of calving styles observed at marine-terminating glaciers, there is no universal law to encompass all calving behavior. Furthermore, uncertainties remain regarding the relative importance of, and the interactions between, different calving mechanisms, as their impact on terminus stability can often vary on different glaciers and at different timescales.

Calving is an episodic process and consists of fracture propagation and the detachment of icebergs following terminus destabilization (Bassis and Jacobs, 2013). Calving styles and iceberg aspect ratio are therefore influenced by longitudinal stress gradients within the glacier, which determine the location and penetration of surface and basal crevasses

(Benn et al., 2007a; Nick et al., 2010). The presence of a proglacial ice mélange in the fjord may provide a small resistive force capable of stabilizing the terminus and suppressing calving during the winter (Amundson et al., 2010; Vieli and Nick, 2011). In the summer, the presence of water in surface crevasses can promote calving by causing the fractures to deepen and produce icebergs (Benn et al., 2007a; Nick et al., 2010; Vieli and Nick, 2011; Cook et al., 2012). Submarine melt and undercutting of the ice cliffs can significantly modify terminus geometry and lead to calving of the unsupported portion of the ice face (O'Leary and Christoffersen, 2013; Cook et al., 2014). Variations in buoyancy conditions at the terminus further alter the force balance and can push the ice margin to flotation, promoting calving through the propagation of basal crevasses. Glacier termini can be forced out of buoyant equilibrium by changes in ice thickness and water depth, which are sensitive to a number of processes such as rapid surface melt or water-level rise, rapid ice motion, and dynamic thinning (Benn et al., 2007b; Nick et al., 2010; Murray et al., 2015).

This study aims to identify the mechanisms controlling calving behavior variability at Rink Isbræ, a major marine terminating glacier in West Greenland. Calving events are documented from a data set of daily terrestrial photographs acquired over the span of five years (2007–2011). A semiquantitative assessment of calving behavior is compiled, including information concerning the relative magnitude, timing, and location of single calving events. From this, the controls on event size, inter-event intervals, as well as any spatial patterns in calving activity are determined.

Study Site

Rink Isbræ (71°45′N, 51°40′W) terminates in a narrow fjord in the Uummannaq district of West Greenland (Fig. 1). With a drainage basin size of 30,000 km^2, Rink Isbræ drains ~3.5% of the Greenland Ice Sheet (Rignot and Kanagaratnam, 2006) through a 4.5-km-wide terminus. The front position has remained quasi-stable since 2000 (Howat et al., 2010; Box and Decker, 2011; Moon et al., 2014) and no speedup or surface elevation changes were recorded between 2000 and 2009 (McFadden et al., 2011). Surface ice motion averaged 4.5 km a^{-1} for the 2009–2013 period, with intra-annual motion variations of 10% correlated with seasonal terminus position changes, where summertime terminus retreat coincides with speedup, and winter advance with slowdown (Moon et al., 2014). Rignot and Kanagaratnam (2006) measured ice discharge rates of 11.8 km^3 a^{-1} between 2000 and 2005 from the difference between the ice flux at a flux gate (velocities calculated from satellite radar interferometry) and the surface mass balance downglacier of the flux gate.

Bathymetric data of the inner fjord reveal two deep basins reaching over 1000 m below sea level, separated by a 200-m-high submarine moraine ridge, peaking at roughly 600 m below water level, and extending across the fjord about 2 km seaward of the ice margin (Dowdeswell et al., 2014). The water depth at the ice front reaches ~1000 m over the central 2 km of the terminus, and slopes up to 200 m along the sides of the fjord (Rignot et al., 2015). The maximum depth of the ice at the glacier front reaches ~750 m in the midsection of the fjord (Chauché et al., 2014; Rignot et al., 2015). For most of the glacier width, the terminus approaches buoyant equilibrium and forms a floating ice tongue, while the northernmost kilometer of the front is grounded. Subsurface undercutting by submarine melt affects most of the ice front, and the resulting basal cavity extends several hundred meters upglacier from the ice cliffs (Rignot et al., 2015).

Monthly mean surface air temperatures (SATs) measured at the Qaarsut Airport weather station (70°44′N, 52°42′W; 88 m a.s.l.), located in Uummannaq Fjord, ~120 km south of Rink's terminus (Cappelen, 2014) indicate that temperatures over the study period are highest in July (10 °C) and lowest in March (–13.9 °C). The melt season generally lasts from early May until late September. Mean annual temperatures range between –4.0 °C for 2008 and –0.4 °C for 2010 with an average of –2.9 °C for all five years.

Methods

Time-Lapse Cameras

Two 10.2 megapixel digital single-lens reflex (SLR) cameras (Nikon D200) with fixed fo-

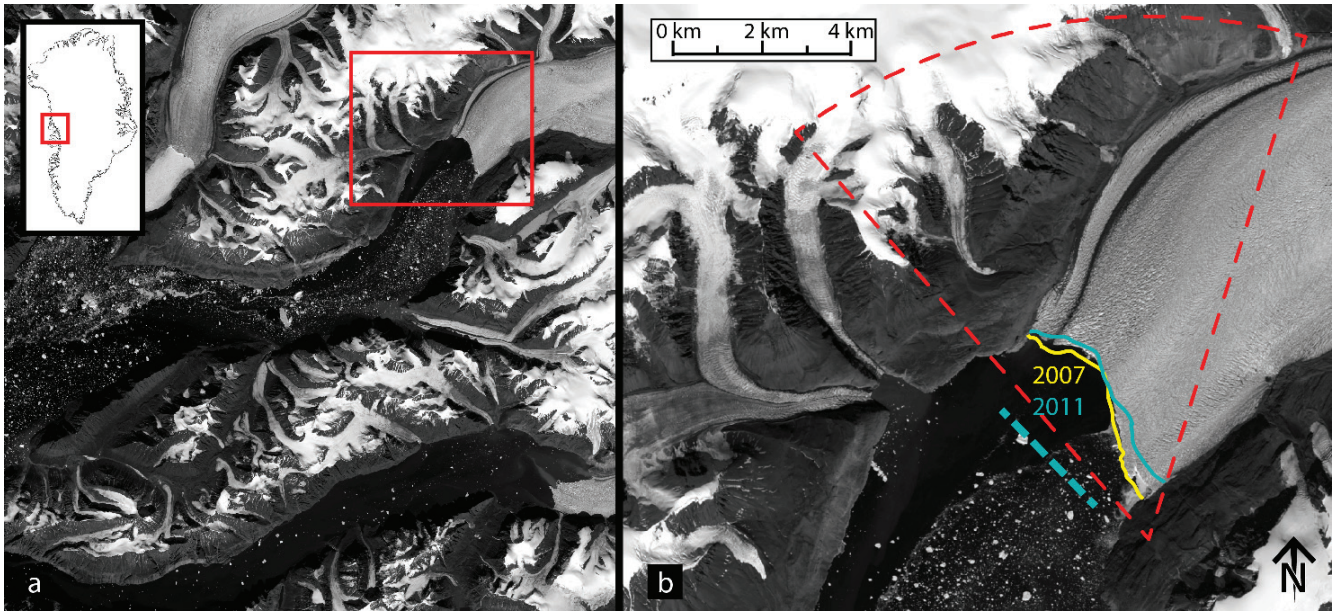

FIGURE 1. Study site. (a) Landsat 7 image (8 July 2014) of Rink Fjord, West Greenland. (b) Rink Isbræ calving front with approximate viewshed of the cameras marked by dashed red lines. Ice front positions are shown for 2007 (yellow) and 2011(blue). The dashed blue line about 2 km down the fjord from the ice margin indicates the position of a 200-m-high transverse submarine moraine ridge.

cal length lenses (Nikkor 20 mm) were installed on the southern side of Rink Fjord (71°42.348′N, 51°38.055′W and 71°42.436′N, 51°37.764′W) overlooking the calving front (Fig. 1). The installation was performed as part of the Extreme Ice Survey. Custom timers developed by the U.S. National Geographic Society's Remote Imaging Laboratory were programmed to take daily photographs at 15:00 UTC (noon local time) between June 2007 and July 2011. The cameras were enclosed in Pelican cases with custom-installed optically neutral plastic windows, and powered with 50 Ah gel cell batteries connected to 10 W solar panels (Ahn and Box, 2010).

The data set for 2010–2011 was acquired by the second camera located about 100 m away from the first location. The view from this camera is therefore different for the last two years of the study, with the southernmost 250 m or so of the glacier front obscured by rocks. Consequently, the 2010–2011 data set is missing some of the calving activity occurring close to the southern margin. The lack of solar illumination during the polar night and camera malfunction in cold temperatures resulted in data gaps of several months during winter. Additional data loss caused by clouds, fog, and rain drops accounts for a loss rate of ~10% for all years of the study period (Table 1). In total 803 images were analyzed.

Calving Event Magnitude Scale

In total, 984 single calving events were documented following a semiqualitative approach where the size and location of each event were determined

TABLE 1

Data set, study periods, and yearly image losses. The high percentage of "other" losses for 2011 is because the camera remained operational during the winter (January–February) when cold temperatures (<–30 °C) caused temporary sticking of the shutter.

Data period (dd.mm.yy)	Days	Yearly images loss due to		Images analysed
		Clouds (%)	Other (%)	
12.06.07–21.10.07	132	10.6	0	118
15.02.08–06.10.08	235	10.6	0	210
03.03.09–08.08.09	159	10.8	0.7	141
31.03.10–20.11.10	236	10.0	3.4	205
28.01.11–21.07.11	182	11.0	19.8	129
Total	944			803

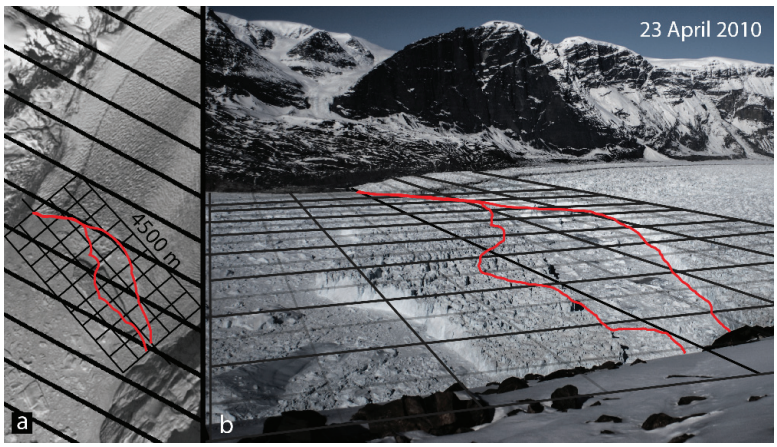

FIGURE 2. (a) Landsat 7 scene from 23 April 2010 with 500 × 500 m grid and digitized position of calving front. (b) Image taken on the same day (15:00 UTC) with approximate grid built based on the Landsat grid. The two red lines indicate the front position before (22 April) and after (23 April), a magnitude 7 event. The size of the calved iceberg is estimated at 1.3 km².

using a grid overlaid over the terminus. The 250 × 250 m cells were built by comparing the location of easily identifiable features on select time-lapse images and the corresponding Landsat 7 (Enhanced Thematic Mapper Plus [ETM+] band 8 panchromatic) scenes acquired on the same day (Fig. 2). The position of the calving front was manually digitized for each daily image and the resulting sequence of vectors was analyzed to identify variations in front geometry. Based on visual observation, events were classified following a nonlinear magnitude scale ranging from 1 to 7, with the relative size of each event and the associated mass loss being approximated based on the number of 250 × 250 m cells implicated in the event (Table 2). Calving event sizes vary from small debris avalanches and isolated blocks that alter ice front geometry but do not result in retreat (magnitude 1), to large events involving nearly the full terminus width (magnitude 7), the largest of which produce massive tabular icebergs over 1 km² in surface area.

Due to the resolution of the images and the effects of perspective, there can be a bias when it comes to comparing the relative magnitude of events occurring close to the camera, compared to those happening on the other side of the fjord, up to 5 km away. Magnitude 1 events can be impossible to identify at the far side of the glacier and under limited or changing light conditions. The presence of ice mélange in the fjord makes it difficult to identify the ice cliffs during winter/spring months, or to pinpoint with precision the day an event occurs.

TABLE 2

Estimated relative contribution to surface area loss for each magnitude. No volume estimates were made as the ice thickness in the various parts of the terminus is unknown.

Magnitude	Grid cells (n)	Iceberg size (km²)	Of all events (%)	Surface area loss (%)
1	<1	~0.0025	73	5
2	<1	0.0025–0.0625	16	7
3	1–2	0.0625–0.125	5.3	10
4	2–4	0.125–0.25	2.2	10
5	4–10	0.25–0.625	1	10
6	10–20	0.625–1.25	0.9	16
7	>20	>1.25	1	42

Results

Event Size Distribution

Calving event sizes show a highly skewed distribution, with a modal magnitude between 1 and 2 on the 1–7 scale (Fig. 3). Of the 984 events documented, 73% are categorized as magnitude 1, while the largest, magnitude 7 events, represent only 1% of all calving activity. Although infrequent, the magnitude 7 events contribute 42% of surface area loss (Table 2). As the major events affect the full-depth of the terminus, their contribution to overall mass loss is more important compared to that of the smallest events that only affect the portion of the ice cliffs above the waterline.

Figure 4 presents the temporal distribution of all events over the entire study period. Events of

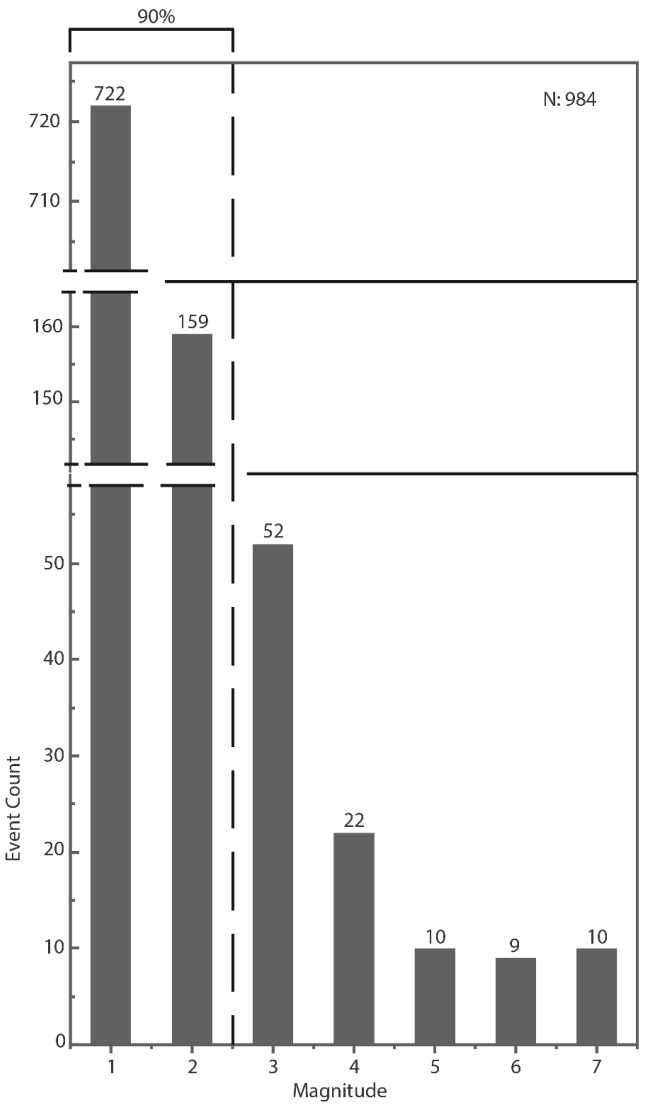

FIGURE 3. Event size distribution. Magnitude 1 and 2 events represent nearly 90% of all events, while large magnitude 5, 6, and 7 events account for ~1% each.

magnitude 5, 6, and 7, here considered to be major events, occur between 3 and 9 times per year with inter-event intervals ranging from a few days to as long as 2 months. Although there are large data gaps in winter observations, major calving events appear to occur at irregular intervals throughout the years with no clear seasonal variation in frequency. Smaller events have significantly shorter repeat intervals, with multiple events occasionally occurring on the same day. Events of magnitude 1, 2, and to some extent, 3, all exhibit a marked increase in frequency in June immediately after the day of ice mélange clearing, reaching a clear peak in July when air temperatures are highest. For two of the five years where data covering the end of the summer period are available (2007 and 2008), the frequency of small events decreases in August–September. Major events appear to lack such clear seasonality.

The change of camera position in 2010 ended up hiding most activity occurring at the southernmost ~250 m of the glacier front from that time onward. In the first three years, 30% of the observed magnitude 1 events occurred within this region. This number dropped to ~7% for the last two years. When the magnitude 1 events occurring in the first 250 m are removed from the total event count for each year, no noticeable difference in calving activity over time exists. This observational bias creates no obvious difference in the frequency of magnitude 2 events and higher as those are larger and remain visible despite the change in camera position.

In the summer, most days experience one or two events greater than magnitude 1. One major drawback of the method used is that the sampling rate does not allow determination of whether the mass lost in the 24 h period between images is the result of one major event or of multiple smaller ones. It would therefore be useful to increase the sampling rate and acquire, for example, hourly photographs during periods of high calving activity. This explains in part the negative relationship between major and minor events, which relates to the fact that fewer small events are detected on days where larger sections of the front collapse, because the large events wipe the minor ones from the record.

Calving Styles and Calving Front Geometry

The spatial variability of calving across the front was analyzed by dividing the terminus into 18 sections of approximately 250 m each and documenting the location of each event (Fig. 5). Magnitude 1–4 events exhibit a strong bimodal distribution with two peaks, one located at kilometer 1, and the other at the limit between kilometers 3 and 4. The significantly stronger peak on the southern side of the fjord may represent a bias introduced by the perspective of the images and possibly missing events further away from the camera. Small events cause the ice cliffs to become irregular and punctuated by small embayments where calving rates are high. Major events of

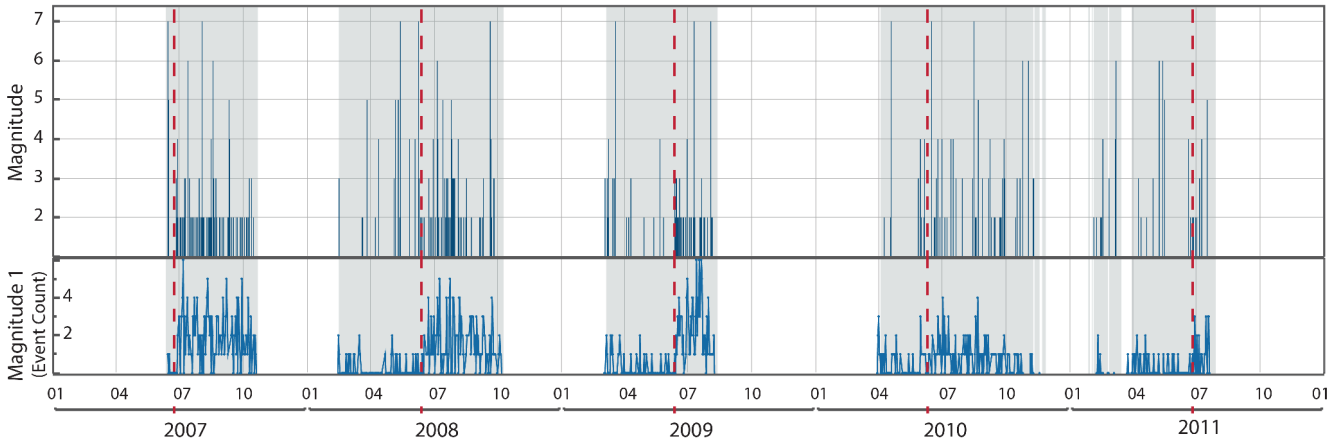

FIGURE 4. Magnitude of daily calving losses for 2007–2011. The red dotted line represents the day of mélange clearing. Events of magnitude 1 are represented separately as they tend to have a much higher frequency with as many as 6 events occurring per day. On days where two larger events occur, their magnitudes are joined in one single value. As this is a nonlinear scale, two distinct magnitude 2 events are not necessarily equivalent to a magnitude 4 event. The gray shaded area indicates the time periods for which data are available.

magnitudes 5–7 on the other hand affect wider portions of the glacier front and often extend up to 4 km, producing an ice margin with a regular, linear, or arcuate geometry. Their distribution is wider, with a shift toward the southern side of the fjord.

Landsat imagery (Fig. 6) shows that major events clearly align with the least crevassed sector of the terminus, which also corresponds to the area with the deepest water and highest ice velocities (Chauché et al., 2014). As the major events appear to be responsible for most of the mass lost through calving (~70% of mass loss), the central sector of the glacier front experiences higher losses than the margins. In contrast, the spatial distribution of low-magnitude calving events coincides with areas closer to the margins, where there are closely spaced crevasses, with a higher calving frequency.

Calving and Ice Mélange Dynamics

In winter, sea ice bonds calved glacier ice in the fjord to produce an ice mélange, which is pushed down the fjord as the terminus advances. The ice mélange thickens throughout the winter and spring, as more icebergs detach from the calving front and become trapped in the sea ice. Time-lapse imagery typically shows the ice mélange at its maximal thickness, with the highest density of trapped icebergs, in March or April. 2011 is the only year with time-lapse data covering the initial formation of the mélange. That year, the fjord remained free of ice until mid-February and the mélange only reached maximum thickness in mid-May. In April, it was thin enough that large cracks, a few kilometers long, fractured the sea ice and revealed some open water. The fjord remained choked with sea ice until late June 2011 (day 176), about 3 weeks later than the previous year. The day of mélange clearing at the terminus can be precisely identified on the time-lapse imagery, which shows a rapid disintegration occurring over the span of one to a few days. The day of clearing is taken as the first day on which icebergs in the fjord move independently from each other.

The glacier terminus typically reaches a maximum position in June, followed by retreat until the end of September and possibly later, although the precise duration of the retreat phase is uncertain due to the lack of data in late fall and winter. There appears to be no strong relation between the timing of the terminus maximum position and that of the mélange clearing in Rink Fjord, although both tend to occur within a few weeks to a month of each other. Indeed, major events (magnitude 5 to 7) are not prevented by the presence of the mélange. On two out of the five years, major events occurred only a few days before the mélange cleared the fjord. As retreat is intimately linked to calving rates, when a major event occurs shortly before the mélange breaks up, the front position recorded immediately preceding that event will be documented as the yearly maximum position.

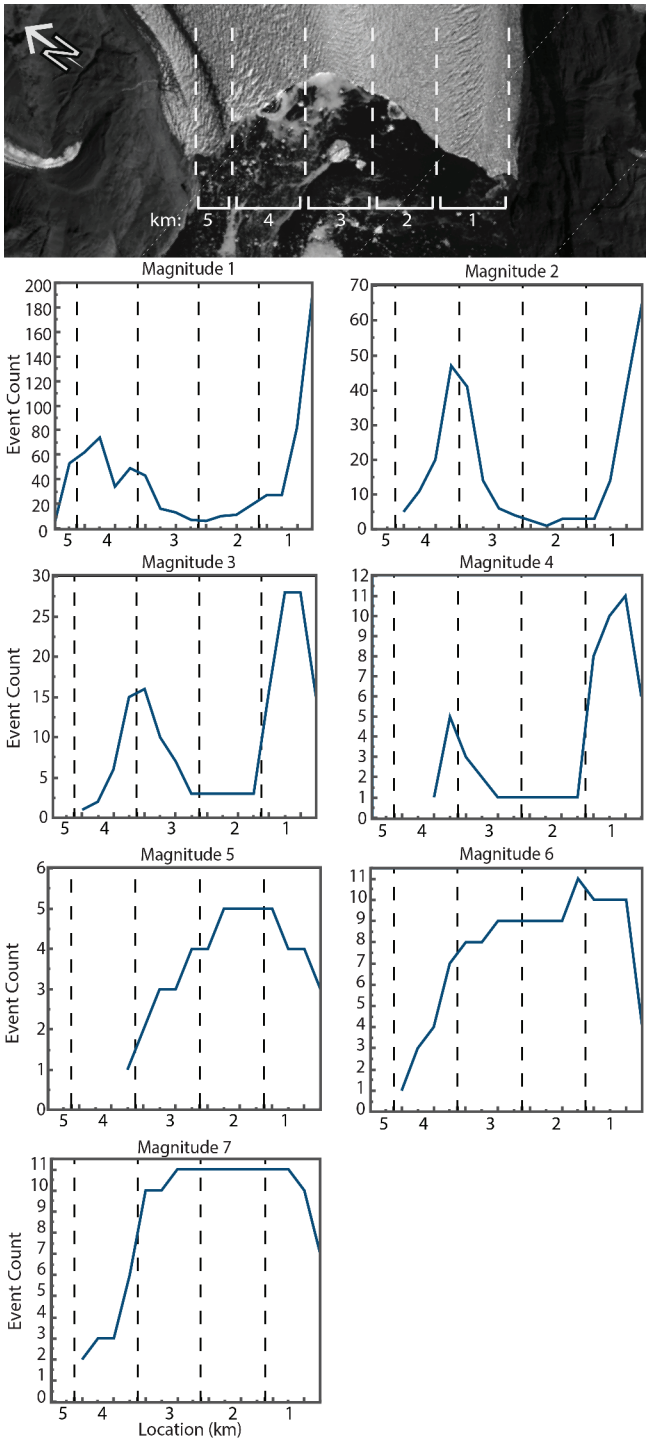

FIGURE 5. Spatial distribution of all logged calving events across the 4.5-km-wide front divided into 18 sections of 250 m each. Notice the different scale for the vertical axis showing event count. The north side of the fjord is on the left.

The rapid increase in calving rates occurring at the time of ice mélange clearing mainly concerns low-magnitude events and affects the more crevassed areas of the front. In four of the five years of study, large embayments in the glacier terminus are observed to form rapidly over a few weeks in June as the mélange disintegrates. The mélange first loses its integrity near the lateral margins of the fjord and calving rapidly picks up at these locations, resulting in retreat (Fig. 7).

Discussion

The time-lapse imagery recovered from Rink Isbræ provides evidence of two different calving styles with distinct temporal and spatial distributions. Small events show an increase in frequency immediately following ice mélange breakup, peak in the summer, and tend to occur preferentially in highly crevassed areas. Major events on the other hand display little seasonal variability and occur at irregular intervals throughout the year. They mostly affect the central, less crevassed section of the front with the highest ice velocities and greatest water depth. The different calving patterns suggest that iceberg production at Rink Isbræ is driven by two distinct mechanisms, each having a specific effect on terminus geometry.

Melt-Driven Calving

Submarine melt has a major impact on terminus stability, and on some glaciers estimates of submarine melt rates are significantly larger than surface melt rates (Motyka et al., 2003, 2011; Rignot et al., 2010; Jenkins, 2011; Enderlin and Howat, 2013). At Rink, Enderlin and Howat (2013) averaged submarine melt rates over the base of the floating ice tongue to produce an estimated melt rate of 2.42 m d^{-1} (with an uncertainty of 3.26 m d^{-1}), while surface melt rates were averaged at a mere 0.0009 m d^{-1} for the 2000–2010 period. Chauché et al. (2014) reported the presence of warm (2.8 ± 0.2 °C) Atlantic water below 400–500 m depth in Rink Fjord. With an ice depth of ~750 m, an extensive section of the glacier front is exposed to this warm water mass, which may enhance submarine melt. Mean rates of volume loss at the terminus were calculated to be 8.0 × 10^6 m^3 d^{-1} from surface and submarine melt combined, and 22.0 × 10^6 m^3 d^{-1} from the calving of icebergs. This volume loss from iceberg calving was calculated from an

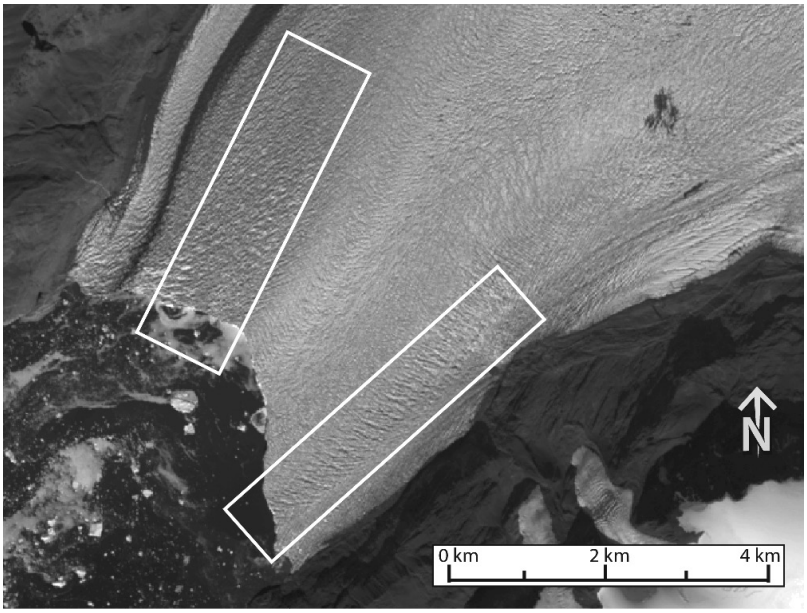

FIGURE 6. Landsat image (20 June 2014) showing the pattern of surface crevasses. The white rectangles indicate the two more crevassed sectors of the terminus.

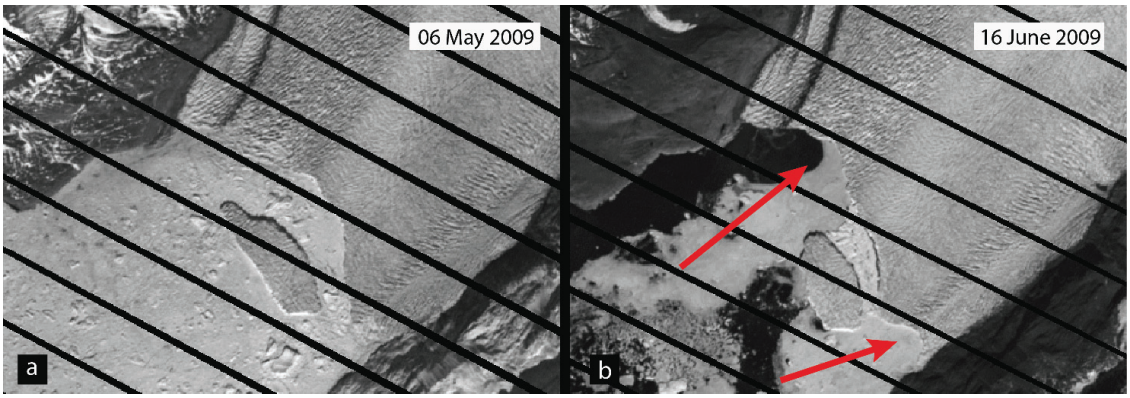

FIGURE 7. Calving front geometry (a) before (6 May 2009) and (b) after (16 June 2009) mélange clearing. Embayments (marked by red arrows) form in locations where calving picks up rapidly following mélange breakup.

estimated ice thickness, and center-line ice velocities determined from feature tracking of optical satellite images (Enderlin and Howat, 2013).

Submarine melting is important as a mass balance term and has been shown to affect calving processes by modifying front geometry. O'Leary and Christoffersen (2013) modeled the effects of submarine melt on the stress patterns at the ice front and found that undercutting of the ice cliffs directly leads to increased calving rates, with larger events occurring with higher melt rates. The sensitivity to undercutting may be heightened when melt is concentrated at the waterline, resulting in the formation of a notch, which leaves a portion of the ice cliffs unsupported and more prone to calving (Cook et al., 2014). This process has been identified as having a direct control on calving rates at a number of lake-terminating glaciers (Kirkbride and Warren, 1997; Benn et al., 2001; Röhl, 2006), and one tidewater glacier on Svalbard (Vieli et al., 2002).

At Rink Isbræ the spatial pattern of the low magnitude events coincides with the main locations of buoyant meltwater upwellings at the terminus. Upwellings are repeatedly observed on the time-lapse imagery between June and September, and they reoccur in the same locations as well-defined areas of turbid water, occasionally pushing brash ice away from the ice cliffs (Fig. 8). These observations are consistent with subglacial wa-

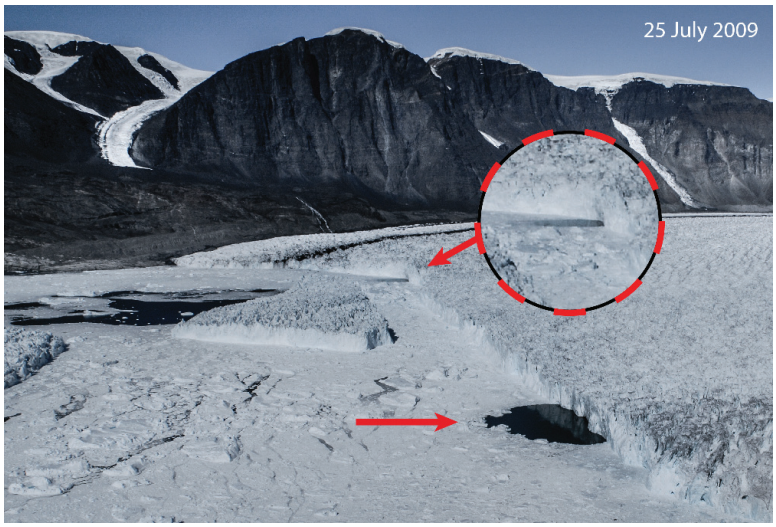

FIGURE 8. Typical locations of glacial meltwater upwellings as observed in all years between June and October.

ter outflow locations predicted by a hydrological model used by Rignot et al. (2015) to calculate water flow direction at the bed of the glacier. Multibeam echo sounding observations additionally revealed that undercutting was most important in the locations of meltwater outflow, with undercutting reaching a maximum of 550 m directly over a meltwater conduit (Rignot et al., 2015). A number of studies have recognized the crucial role of cold freshwater discharge in enhancing submarine melt rates (Motyka et al., 2003; Rignot et al., 2010; Jenkins, 2011; Straneo et al., 2011; Xu et al., 2012; Sciascia et al., 2013). Buoyant freshwater plumes play a crucial role in fjord circulation patterns, driving forced convection as warm bottom water is entrained into the rising plume. This leads to more effective transfer of heat to the ice front and promotes melt. Visual observations at Rink Isbræ suggest that the low magnitude events tend to occur preferentially near meltwater conduits, where undercutting rates are at their highest. Calving rates peak in July, coinciding with higher air temperatures and enhanced meltwater production, and decrease at the end of the summer as temperatures and surface melt drop. It is noteworthy, however, that the same spatial pattern also characterizes winter calving, when submarine melt rates are at their lowest, which indicates that undercutting is not the only mechanism driving calving, and may simply act as a facilitator

Low magnitude events also tend to occur in the highly crevassed areas of the terminus. We therefore suggest that preexisting crevasses advected from regions of high tensile stresses further upglacier provide points of weakness along which iceberg detachment is more likely to occur. Although a highly fractured terminus is more prone to calving, additional forces may be necessary to break the equilibrium and trigger calving events (Bassis and Jacobs, 2013). Undercutting may be considered as an additional perturbation promoting the detachment of bergs from an already fractured front. The input of meltwater into surface crevasses has also been proposed to act as an enhancing factor as it can lead to hydrofracturing that can cause fractures to deepen and potentially propagate through the full thickness of the glacier and lead to calving (van der Veen, 1998, 2007; Benn et al., 2007b; Vieli and Nick, 2011; Cook et al., 2012). Together with undercutting, the presence of more surface meltwater in the summer months could also contribute to the seasonal pattern of low magnitude events.

Mechanically Driven Calving

Submarine melt and undercutting of the ice front affect both grounded and floating termini as they lead to grounding line retreat as well as thinning of floating sections (Rignot et al., 2010; Straneo et al., 2010; Motyka et al., 2011; Seale et al., 2011; Münchow et al., 2014). For buoyant glacier tongues, the ice may be out of hydrostatic equilibrium at the grounding line, resulting in upward-di-

rected torque forces (Warren et al., 2001; Boyce et al., 2007; Murray et al., 2015). Reduction in the ice surface elevation or advance of the terminus into deeper water can result in an increase of "super-buoyancy," which may trigger fracture propagation and calving (Benn et al., 2007b; Nick et al., 2009).

Several processes can drive the terminus out of buoyant equilibrium, including rapid thinning due to surface melt (Warren et al., 2001), rapid water-level rise (Boyce et al., 2007), enhanced ice flow forcing the terminus to advance into deeper water, and dynamic thinning (Murray et al., 2015). The first two processes can be ruled out for Rink Isbræ as they apply to warm environments with high surface melt rates, and lacustrine systems where small short-term perturbations in lake level lead to rapid increases in water depth. Bathymetric data reveal no significant slope change at the terminus (Rignot et al., 2015), suggesting that water depth remains relatively constant as the glacier advances into the fjord. It is possible that super-buoyant conditions develop as the result of dynamic thinning, during which longitudinal extension reduces ice thickness below flotation before hydrostatic equilibrium can be restored by uplift of the front.

Thinning by dynamic adjustment occurs in response to increases in ice velocities and the resulting variations in longitudinal stress gradients (Pfeffer, 2007; Nick et al., 2009). Velocity variations at Rink Isbræ are correlated with seasonal changes in front position, with increased ice motion occurring during summertime retreat (Howat et al., 2010; Moon et al., 2014). The same was also observed at Jakobshavn Isbræ where seasonal acceleration is hypothesized to occur in response to a reduction in backstress brought on by terminus retreat (Joughin et al., 2008a, 2008c). Using a numerical ice-flow model, Nick et al. (2009) showed that outlet glaciers adjust rapidly to changing boundary conditions at the ice margin in response to variations in longitudinal stress gradients. Through the transfer of longitudinal stresses, a perturbation at the terminus such as a reduction in backstress due to calving-driven retreat, may trigger an immediate velocity increase up to 20 km upglacier. Large calving events, or the loss of a portion of a floating ice tongue can therefore substantially modify the longitudinal force balance at the terminus, and lead to acceleration, stretching, and dynamic thinning (Joughin et al., 2004, 2008b; Thomas, 2004; Howat et al., 2005; Nettles et al., 2008; Nick et al., 2009; Vieli and Nick, 2011). The yearly fluctuations in front position (400–1000 m) observed at Rink may also modify stress patterns and explain the 10% seasonal velocity variations. Extensional flow and the associated dynamic thinning are therefore likely to increase buoyancy near the calving front. Smaller surface slope gradients additionally allow a larger area of the front to thin to flotation which increases the area of the terminus affected by buoyancy variations and can promote further retreat (McFadden et al., 2011). Buoyancy conditions at the terminus therefore depend on its geometry, including ice thickness and surface slope, as well as bed topography.

The time-lapse imagery at Rink Isbræ provides evidence of the terminus being forced out of buoyant equilibrium. On several occasions, waterline notches were observed to be raised progressively above water level, indicating uplift of the terminus in response to buoyant forces (cf. Benn et al., 2007b; James et al., 2014; Murray et al., 2015). Back-tilting of the front was observed immediately preceding a few major calving events resulting in the detachment of tabular icebergs. For example, in July 2008, the front was observed to rotate over a period of a week, accelerating progressively until failure occurred about 300 m further upglacier, resulting in a magnitude 5 calving event (Fig. 9). This process was observed to occur two to four times per year, in July and August, and always preceded the detachment of large tabular icebergs by a few days to up to a week. The lifting of the waterline notch during summer months provides evidence for flexure at the front which occurs when the terminus thins below its flotation thickness. The same mechanism of ice front rotation was observed to lead to major calving events at Helheim Glacier where buoyant flexure caused a large surface depression, or flexion zone, to form downglacier of the grounding line, and calving occurred through the propagation of basal crevasses (James et al., 2014; Murray et al., 2015). Although no flexion zone was directly observed at Rink, the progressive uplift of the ice cliffs suggests that calving occurred in a similar fashion, through the propagation of basal crevasses. Tabular icebergs tend to detach in the midsection of the ice margin. Due to deeper water and higher ice ve-

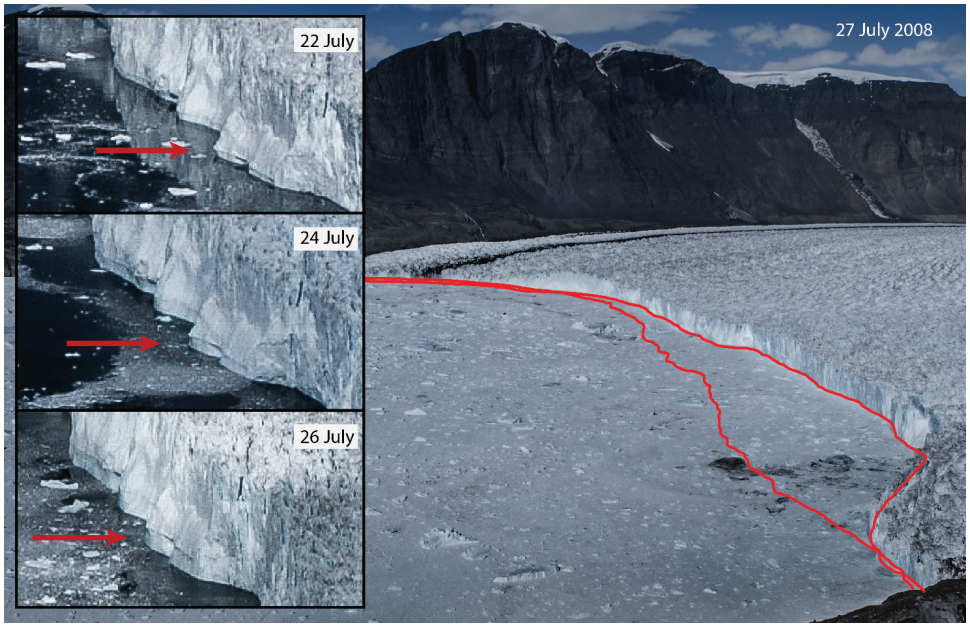

FIGURE 9. A notch appears above the waterline on 22 July 2008 and is raised increasingly higher until a magnitude 5 event on 27 July leads to a ~100 m (width-averaged) retreat of the front.

locities, the center has a greater tendency for extension and flotation, promoting the large, full-depth, mechanically driven calving events. The contrasting calving patterns affecting the areas near the margins could be explained by the variability in buoyancy conditions across the terminus, with grounded areas tending to experience smaller, and more frequent, calving activity.

Frequently, major calving events occur without any signs of back-tilting. This may be because a minimum amount of rotation, too small to be recorded on the time-lapse imagery, is sufficient to cause large basal crevasses to propagate to the surface and lead to calving. The response of the terminus to variations in buoyancy may essentially depend on how the terminus manages to accommodate the resulting changes in the force balance. The determining factor may therefore be how quickly the terminus approaches flotation, and how quickly it compensates for it. According to theory, progressively increasing upward-bending forces can be accommodated by ice creep, but rapid perturbations are more likely to lead to mechanical failure, fracture propagation, and calving (Benn et al., 2007b; Boyce et al., 2007). Another possibility is that rotation is not a prerequisite for calving and that in some cases bergs breakoff through progressive rift propagation induced by longitudinal stretching. Where neither rifts nor rotation are visible, what appears to be one major event might instead be the result of multiple smaller events that are not recorded on the time-lapse imagery due to the daily sampling rate examined here.

The fact that the detachment of large tabular icebergs is sporadic and displays only a weak seasonal signal (i.e., major events occur at irregular intervals throughout the year with no clear seasonality), indicates that the terminus remains close to flotation throughout the year. However, enhanced melt in the summer (both basal and surface), as well as dynamic thinning, has the potential to significantly modify buoyancy conditions at the terminus. This would explain the seasonal behavior of winter advance and summer retreat. As the major events are responsible for most of the mass lost through calving, they must also, together with frontal melt, be accountable for some of the seasonal length fluctuations of the floating ice tongue.

Ice Mélange Dynamics

Ice mélange has been observed to act like a transient thin ice tongue that can generate a small resistive force (or backstress) that stabilizes the front and limits calving (Sohn et al., 1998; Reeh et al., 2001; Joughin et al., 2008c; Amundson et al., 2010; Howat et al., 2010; Herdes et al., 2012; Walter et al., 2012; Nick et al., 2013). Both oceanic and atmospheric conditions have a major impact on sea ice concentrations and the integrity of ice mélange, which has been reported as being an important influence on

the timing of calving events, as well as a contributor to the seasonal advance and retreat cycle.

Cook et al. (2014) modeled the effect of ice mélange on longitudinal stress gradients and found that realistic values of backstress were insufficient to significantly influence the crevasse patterns around the terminus. Although the mélange might be too weak structurally to influence the propagation of fractures, Amundson et al. (2010) suggested that it may have a stabilizing effect by preventing icebergs from overturning and drifting away from the terminus. This effect is clearly visible in the winter when the mélange effectively stabilizes calved ice, counteracting rotational forces that would otherwise lead to capsizing. The rapid increase in calving rates in the highly crevassed areas of the front immediately following mélange breakup suggests that the backstress may indeed prevent the already fractured areas of the front from disintegrating and the icebergs from drifting away. As with the submarine melt and undercutting, the loss of backstress due to ice mélange breakup in June may represent another mechanism capable of providing additional perturbations leading to the detachment of icebergs from an already fractured front. As calving picks up at the margins, the middle section of the front continues to advance, forming a large headland that extends as far as ~1 km farther out into the fjord. The advance of the headland is rather short-lived and it quickly disintegrates in a series of larger events, returning the front to a more linear geometry in a matter of weeks. Although it is not possible to establish causality between the two, the rapid retreat near the lateral margins may conceivably affect the middle section of the terminus by reducing lateral drag.

Separating the influence of both melt-induced processes (undercutting and hydrofracturing), and ice mélange variations on terminus behavior is not straightforward. Although mean surface air temperatures indicate that the melt season starts in May, calving rates remain low until the ice mélange clears the fjord, which points to sea ice conditions as a controlling mechanism. However, the frequency of small calving events peaks in July (Fig. 4), coinciding with the highest air temperatures, and drops slightly near the end of the summer, suggesting an influence of surface meltwater runoff. Although data are not available for all years, the minimum front position is generally observed in late fall or in the winter, indicating that calving continues after sea and air temperatures drop below freezing. It is therefore possible that the progressive buildup of sea ice in the fjord is the main factor suppressing small calving events in the winter, and until mélange clearing in June-July.

Conclusion

The time-lapse data set covering the terminus at Rink Isbræ allows for the detailed characterization of calving activity and the identification of individual calving events. The high spatial resolution of the photographs, as well as the higher frequency of observations, offer a level of detail not possible from conventional satellite or airborne imaging. Results show two distinct calving styles with different temporal and spatial footprints. Small magnitude events tend to occur near the margins and are concentrated in highly crevassed areas where the ice is more likely grounded. Events in this first category experience sudden increases in frequency immediately following ice mélange clearing and peak in July during maximum meltwater runoff. Their spatial distribution is correlated with the location of upwellings where submarine melt rates and undercutting are expected to be at their highest. We suggest that low magnitude events occur in fractured areas of the terminus where melt undercutting, and potentially hydrofracturing, destabilize the preexisting crevasses and lead to frequent small iceberg detachment. In winter, the presence of ice mélange is suspected to prevent icebergs from drifting away from the already fractured front. It is suggested that closer to the margins the ice is too fractured to support the advance of a floating ice tongue. Those areas are instead frequently eroded due to their sensitivity to melt and runoff. Although the impact of small events is limited in terms of scale and resulting mass loss, they play a crucial role in glacier dynamics by modifying front geometry.

The second calving style is characterized by the sporadic detachment of kilometer-sized tabular icebergs, which is not prevented by the presence of the ice mélange over the winter months. Major calving events mainly affect the midsection of the glacier terminus, where deep water and higher ice velocities bring the ice margin toward flotation. Backward rotation of the terminus was observed

immediately preceding some major calving events. It is therefore suggested that the large full-depth calving events occur in response to mechanical forcing where failure and rift propagation are induced by longitudinal stretching and buoyant flexure. Due to their spatial extent, the major events are responsible for most of the mass lost through calving and as a result they substantially modify front geometry. The seasonal growth and decay of the floating ice tongue, and the associated variations in backstress, are additionally suspected to modify longitudinal stress gradients and cause seasonal velocity variations (Howat et al., 2010; Moon et al., 2014). Buoyancy-driven positive feedbacks between calving and dynamic thinning therefore provide an effective mechanism for terminus retreat.

Overall, the spatial and temporal variability of calving styles observed at Rink Isbræ seems to be related to terminus geometry, including crevasse density, ice thickness, and fjord topography. Longitudinal stretching as well as buoyancy conditions can be considered as the primary controls on terminus behavior. Undercutting by submarine melt and hydrofracturing, both intensified by increased meltwater runoff, act as enhancing mechanisms. The backstress provided by the ice mélange is, on the other hand, a mitigating factor, limiting calving in the winter. The variability in calving behavior emerging from the evidence reviewed in this study shows that Rink Isbræ experiences two different calving styles concurrently. It is suggested that the low magnitude events are melt-driven, whereas the major ones are mechanically driven and occur mainly in response to buoyant-flexure. This indicates that one single glacier can exhibit distinct calving styles resulting from the interaction between different mechanisms, as is likely to be the case at other Greenland outlet glaciers. The relative importance of these processes may vary and some glaciers appear to be dominated by buoyant calving (e.g., Helheim Glacier [James et al., 2014]), and others by melt undercutting (e.g., Store Glacier [Chauché et al., 2014]). Other processes such as longitudinal extension and transverse rifting may be important at other outlets. Determining the interplay between each of these processes at various sites will require additional studies. Rink Isbræ exhibits relatively little long-term variation in terminus position over the study period, so these observations provide a control case documenting the processes driving iceberg calving under conditions unaffected by rapid terminus retreat seen at many other Greenland glaciers.

Acknowledgments

This project was part of CRIOS (Calving Rates and Impact on Sea Level), funded by the ConocoPhillips Lundin Northern Areas Research Program. Thanks are due to Nina Kirchner for support for Medrzycka at the University of Stockholm, and the Natural Sciences and Engineering Research Council of Canada for funding.

References Cited

Ahn, Y., and Box, J. E., 2010: Glacier velocities from time-lapse photos: technique development and first results from the Extreme Ice Survey (EIS) in Greenland. *Journal of Glaciology*, 56(198): 723–734.

Amundson, J. M., Fahnestock, M., Truffer, M., Brown, J., Lüthi, M. P., and Motyka, R. J., 2010: Ice mélange dynamics and implications for terminus stability, Jakobshavn Isbræ, Greenland. *Journal of Geophysical Research*, 115: F01005.

Bassis, J. N., and Jacobs, S., 2013: Diverse calving patterns linked to glacier geometry. *Nature Geoscience*, 6: 833–836.

Benn, D. I., Wiseman, S., and Hands, K. A., 2001: Growth and drainage of supraglacial lakes on debris-mantled Ngozumpa Glacier, Khumbu Himal, Nepal. *Journal of Glaciology*, 47(159): 626–638.

Benn, D. I., Hulton, N. R. J., and Mottram, R. H., 2007a: "Calving laws," "sliding laws," and the stability of tidewater glaciers. *Annals of Glaciology*, 46: 123–130.

Benn, D. I., Warren, C. R., and Mottram, R. H., 2007b: Calving processes and the dynamics of calving glaciers, *Earth-Science Reviews*, 82: 143–179.

Box, J. E., and Decker, D. T., 2011: Greenland marine-terminating glacier area changes: 2000–2010. *Annals of Glaciology*, 52(59): 91–98.

Boyce, E. S., Motyka, R. J., and Truffer, M., 2007: Flotation and retreat of a lake-calving terminus, Mendenhall Glacier, southeast Alaska, USA. *Journal of Glaciology*, 53(181): 211–224.

Cappelen, J. (ed.), 2014: *Weather Observations from Greenland 1958–2013, Observation Data with Description.* Copenhagen: Danish Meteorological Institute, Technical Report 14-08.

Chapuis, A., and Tetzlaff, T., 2014: The variability of tidewater-glacier calving: origin of event-size and interval distributions. *Journal of Glaciology*, 60(222): 622–634.

Chauché, N., Hubbard, A., Gascard, J.-C., Box, J. E., Bates, R., Koppes, M., Sole, A., Christoffersen P., and Patton, H., 2014: Ice-ocean interaction and calving front morphology at two west Greenland tidewater outlet glaciers. *The Cryosphere*, 8: 1457–1468.

Cook, S., Zwinger, T., Rutt, I. C., O'Neel, S., and Murray, T., 2012: Testing the effect of water in crevasses on a physically based calving model. *Annals of Glaciology*, 53(60): 90–96.

Cook, S., Rutt, I. C., Murray, T., Luckman, A., Zwinger, T., Selmes, N., Goldsack A., and James, T. D., 2014: Modelling environmental influences on calving at Helheim Glacier in eastern Greenland. *The Cryosphere*, 8: 827–841.

Dowdeswell, J. A., Hogan, K. A., O'Cofaigh, C., Fugelli, E. M. G., Evans, J., and Noormets, R., 2014: Late Quaternary ice flow in a West Greenland fjord and cross-shelf trough system: submarine landforms from Rink Isbrae to Uummannaq shelf and slope. *Quaternary Science Reviews*, 92: 292–309.

Enderlin, E. N., and Howat, I. M., 2013: Submarine melt rate estimates for floating termini of Greenland outlet glaciers (2000–2010). *Journal of Glaciology*, 59(213): 67–75.

Herdes, E., Copland, L., Danielson, B., and Sharp, M., 2012: Relationships between iceberg plumes and sea-ice conditions on northeast Devon Ice Cap, Nunavut, Canada. *Annals of Glaciology*, 53(60): 1–9.

Howat, I. M., Joughin, I., Tulaczyk, S., and Gogineni, S., 2005: Rapid retreat and acceleration of Helheim Glacier, east Greenland. *Geophysical Research Letters*, 32: L22502, doi http://dx.doi.org/10.1029/2005GL024737.

Howat, I. M., Box, J. E., Ahn, Y., Herrington A., and McFadden, E. M., 2010: Seasonal variability in the dynamics of marine-terminating outlet glaciers in Greenland. *Journal of Glaciology*, 56(198): 601–613.

James, T. D., Murray, T., Selmes, N., Scharrer, K., and O'Leary, M., 2014: Buoyant flexure and basal crevassing in dynamic mass loss at Helheim Glacier. *Nature Geoscience*, 7: 593–596.

Jenkins, A., 2011: Convection-driven melting near the grounding lines of ice shelves and tidewater glaciers. *Journal of Physical Oceanography*, 41(12): 2279–2294.

Joughin, I., Abdalati, W., and Fahnestock, M., 2004: Large fluctuations in speed on Greenland's Jakobshavn Isbræ glacier. *Nature*, 432: 608–610.

Joughin, I., Das, S. B., King, M. A., Smith, B. E., Howat, I. M., and Moon, T., 2008a: Seasonal speedup along the western flank of the Greenland Ice Sheet. *Science*, 320: 781–783.

Joughin, I., Howat, I., Alley, R. B., Ekstrom, G., Fahnestock, M., Moon, T., Nettles, M., Truffer, M., and Tsai, V. C., 2008b: Ice-front variation and tidewater behaviour on Helheim and Kangerdlugssuaq Glaciers, Greenland. *Journal of Geophysical Research*, 113: F01004, doi http://dx.doi.org/10.1029/2007JF000837.

Joughin, I., Howat, I. M., Fahnestock, M., Smith, B., Krabil, W., Alley, R. B., Stern H., and Truffer, M., 2008c: Continued evolution of Jakobshavn Isbræ following its rapid speedup. *Journal of Geophysical Research*, 113: F04006, doi http://dx.doi.org/10.1029/2008JF001023.

Kirkbride, M. P., and Warren, C. R., 1997: Calving processes at a grounded ice cliff. *Annals of Glaciology*, 24: 116–121.

McFadden, E. M., Howat, I. M., Joughin, I., Smith, B. E., and Ahn, Y., 2011: Changes in the dynamics of marine terminating outlet glaciers in west Greenland (2000–2009). *Journal of Geophysical Research*, 116: F02022, doi http://dx.doi.org/10.1029/2010JF001757.

Moon, T., Joughin, I., Smith, B., van den Broeke, M. R., van de Berg, W. J., Noël, B., and Usher, M., 2014: Distinct patterns of seasonal Greenland glacier velocity. *Geophysical Research Letters*, 41: 7209–7216.

Motyka, R. J., Hunter, L., Echelmeyer, K. A., and Connor, C., 2003: Submarine melting at the terminus of a temperate tidewater glacier, LeConte Glacier, Alaska, USA. *Annals of Glaciology*, 36: 57–65.

Motyka, R. J., Truffer, M., Fahnestock, M., Mortensen, J., Rysgaard, S., and Howat, I., 2011: Submarine melting of the 1985 Jakobshavn Isbræ floating tongue and the triggering of the current retreat. *Journal of Geophysical Research*, 116: F01007, doi http://dx.doi.org/10.1029/2009JF001632.

Münchow, A., Padman, L., and Fricker, H. A., 2014: Interannual changes of the floating ice shelf of Petermann Gletscher, North Greenland, from 2000 to 2012. *Journal of Glaciology*, 60(221): 489–499.

Murray, T., Selmes, N., James, T. D., Edwards, S., Martin, I., O'Farrell, T., Aspey, R., Rutt, I., Nettles, M., and Baugé, T., 2015: Dynamics of glacier calving at the ungrounded margin of Helheim Glacier, southeast Greenland. *Journal of Geophysical Research*, 120: doi http://dx.doi.org/10.1002/2015JF003531.

Nettles, M., Larsen, T. B., Elósegui, P., Hamilton, G. S., Stearns, L. A., Ahlstrøm, A. P., Davis, J. L., Andersen, M. L., de Juan, J., Khan, S. A., Stenseng, L., Ekström, G., and Forsberg, R., 2008: Step-wise changes in glacier flow speed coincide with calving and glacial earthquakes at Helheim Glacier, Greenland. *Geophysical Research Letters*, 35: L24503, doi http://dx.doi.org/10.1029/2008GL036127.

Nick, F. M., Vieli, A., Howat, I. M., and Joughin, I., 2009: Large-scale changes in Greenland outlet glacier dynamics triggered at the terminus. *Nature Geoscience*, 2: 110–114.

Nick, F. M., van der Veen, C. J., Vieli, A., and Benn, D. I., 2010: A physically based calving model applied to marine outlet glaciers and implications for the glacier dynamics. *Journal of Glaciology*, 56(199): 781–794.

Nick, F. M., Vieli, A., Andersen, M. L., Joughin, I., Payne, A., Edwards, T. L., Pattyn, F., and van de Wal, R. S. W., 2013: Future sea-level rise from Greenland's main outlet glaciers in a warming climate. *Nature*, 497: 235–238.

O'Leary, M., and Christoffersen, P., 2013: Calving on tidewater glaciers amplified by submarine frontal melting. *The Cryosphere*, 7: 119–128.

O'Neel, S., Echelmeyer, K. A., and Motyka, R. J., 2003: Short-term variations in calving of a tidewater glacier: LeConte Glacier, Alaska, USA. *Journal of Glaciology*, 49(167): 587–598.

O'Neel, S., Pfeffer, W. T., Krimmel, R., and Meier, M., 2005: Evolving force balance at Columbia Glacier, Alaska, during its rapid retreat. *Journal of Geophysical Research*, 110: F03012, doi http://dx.doi.org/10.1029/2005JF000292.

O'Neel, S., Marshall, H. P., McNamara, D. E., and Pfeffer, W. T., 2007: Seismic detection and analysis of icequakes at Columbia Glacier, Alaska. *Journal of Geophysical Research*, 112: F03S23, doi http://dx.doi.org/10.1029/2006JF000595.

Pfeffer, W. T., 2007: A simple mechanism for irreversible tidewater glacier retreat. *Journal of Geophysical Research*, 112: F03S25, doi http://dx.doi.org/10.1029/2006JF000590.

Reeh, N., Højmark Thomsen, H., Higgins A. K., and Weidick, A., 2001: Sea ice and the stability of north and northeast Greenland floating glaciers. *Annals of Glaciology*, 33: 474–480.

Rignot, E., and Kanagaratnam, P., 2006: Changes in the velocity structure of the Greenland Ice Sheet. *Science*, 311: 986–990.

Rignot, E., Kopped, M., and Velicogna, I., 2010: Rapid submarine melting of the calving faces of West Greenland glaciers. *Nature Geoscience*, 3: 187–191.

Rignot, E., Fenty, I., Xu, Y., Cia, C., and Kemp C., 2015: Undercutting of marine-terminating glaciers in West Greenland. *Geophysical Research Letters*, 42: 5909–5917.

Röhl, L., 2006: Thermo-erosional notch development at fresh-water-calving Tasman Glacier, New Zealand. *Journal of Glaciology*, 52(177): 203–213.

Sciascia, R., Straneo, F., Cenedese, C., and Heimback, P., 2013: Seasonal variability of submarine melt rate and circulation in an East Greenland fjord. *Journal of Geophysical Research*, 118: 2492–2506.

Seale, A., Christoffersen, P., Mugford, R. I., and O'Leary, M., 2011: Ocean forcing of the Greenland Ice Sheet: calving fronts and patterns of retreat identiffed by automatic satellite monitoring of eastern outlet glaciers. *Journal of Geophysical Research*, 116: F03013, doi http://dx.doi.org/10.1029/2010JF001847.

Sohn, H. G., Jezek, K. C., and van der Veen, C. J., 1998: Jakobshavn Glacier, West Greenland: 30 years of spaceborne observations. *Geophysical Research Letters*, 25(14): 2699–2702.

Straneo, F., Hamilton, G. S., Sutherland, D. A., Stearns, L. A., Davidson, F., Hammill, M. O., Stenson, G. B., and Rosing-Asvid, A., 2010: Rapid circulation of warm subtropical waters in a major glacial fjord in East Greenland. *Nature Geoscience*, 3: 182–186.

Straneo, F., Curry, R. G., Sutherland, D. A., Hamilton, G. S., Cenedese, C., Våge, K., and Stearns, L. A., 2011: Impact of fjord dynamics and glacial runoff on the circulation near Helheim Glacier. *Nature Geoscience*, 4: 322–327.

Thomas, R. H., 2004: Force-perturbation analysis of recent thinning and acceleration of Jakobshavn Isbræ, Greenland. *Journal of Glaciology*, 50(168): 57–66.

van der Veen, C. J., 1998: Fracture mechanics approach to penetration of surface crevasses on glaciers. *Cold Regions Science and Technology*, 27: 31–47.

van der Veen, C. J., 2007: Fracture propagation as means of rapidly transferring surface meltwater to the base of glaciers. *Geophysical Research Letters*, 34: L01501, doi http://dx.doi.org/10.1029/2006GL028385.

Vieli, A., and Nick, F. M., 2011: Understanding and modelling rapid dynamic changes of tidewater outlet glaciers: issues and implications. *Surveys in Geophysics*, 32: 437–458.

Vieli, A., Jania, J., and Kolondra, L., 2002: The retreat of a tidewater glacier: observations and model calculations on Hansbreen, Spitsbergen. *Journal of Glaciology*, 48(163): 592–600.

Walter, J. I., Box, J. E., Tulaczyk, S., Brosky, E. E., Howat, I. M., Ahn, Y., and Brown, A., 2012: Oceanic mechanical forcing of a marine-terminating Greenland glacier. *Annals of Glaciology*, 53(60): 181–192.

Warren, C., Benn, D., Winchester, V., and Harrison, S., 2001: Buoyancy-driven lacustrine calving, Glaciar Nef, Chilean Patagonia. *Journal of Glaciology*, 47(156): 135–146.

Xu, Y., Rignot, E., Menemenlis, S., and Koppes, M., 2012: Numerical experiments on subaqueous melting of Greenland tidewater glaciers in response to ocean warming and enhanced subglacial discharge. *Annals of Glaciology*, 53(60): 229–234.

MS submitted 26 August 2015
MS accepted 14 December 2015